

# Evaluation of Molecular Orientation in Injection Molded Parts with Microscale Features by Raman Spectroscopy

Osamu Murakami,<sup>1</sup> Kazushi Yamada,<sup>2</sup> Masaya Kotaki,<sup>2</sup> Hiroyuki Hamada<sup>2</sup>

<sup>1</sup>Advanced Technology R&D Center, Mitsubishi Electric Corporation 8-1-1, Amagasaki City, Hyogo 661-8661, Japan

<sup>2</sup>Department of Advanced Fibro-Science, Kyoto Institute of Technology, Sakyo-ku, Kyoto 606-8585, Japan

Received 22 February 2008; accepted 8 October 2008

DOI 10.1002/app.29607

Published online 9 February 2009 in Wiley InterScience (www.interscience.wiley.com).

**ABSTRACT:** Molecular orientation of polycarbonate (PC) in injection-molded parts with microscale features was characterized by means of polarized Raman spectroscopy, and the relationship between microstructure and replication was discussed. The microscale feature size of continuous v-groove was 20  $\mu\text{m}$  in depth and 50  $\mu\text{m}$  in width. PC injection-molded parts were molded with various molding conditions. The molecular orientation distribution along flow direction on the cross-section of molding parts were evaluated by the intensity ratio of the bands at 635 to 703  $\text{cm}^{-1}$  ( $I_{635}/I_{703}$ ) in the Raman spectra. Molecular orientation along

the flow direction inside the v-groove was higher than that of the core and the opposite surface region. In particular, the highest molecular orientation was at the surface of the v-groove. Among the injection molding conditions, the mold temperature showed significant effect on the molecular orientation and replication. Higher mold temperature caused high replication and low molecular orientation. © 2009 Wiley Periodicals, Inc. *J Appl Polym Sci* 112: 1607–1614, 2009

**Key words:** injection molding; microscale features; molding; Raman spectroscopy; orientation

## INTRODUCTION

Recently, there has been a rapid increase in the production of polymer components for microengineering applications with micro or nanostructured surfaces such as compact disk, digital versatile disk, light guide plate, microlens array, MEMS, micromachine, and microsensor. These products have microscale feature on the surface of molding parts.<sup>1</sup> The actual volume production requires low-cost mass-production methods. Among the available molding processes for microscale feature replication, injection molding is considered the most efficient method in terms of short cycle time, high degree of automation, and high accuracy and consistency.<sup>2</sup> In particular, microscale features are responsible for controlling visible or laser light as designed for optical devices. To produce plastics parts of microscale features with high accuracy by injection molding, some studies have revealed that the relationship between molding conditions and replication.<sup>3–5</sup>

Evaluation of the microstructure of injection-molded parts with microscale features is important to understand the filling mechanism in the microscale features. In addition, the microstructure is related to the product performance of many optical devices. However, the microstructures of injection-

molded parts with microscale features have not been fully understood. As for macroscopic injection-molded parts, microstructures of injection molded parts had been studied by various techniques. The investigation on microstructure and molecular orientation in injection-molded parts can be approached by optical birefringence, infrared spectroscopy (IR), and X-ray scattering (SAXS and WAXS). However, birefringence using microscope and IR provide the average information in a certain area/thickness of the injection-molded parts for orientation of a molecular segment because of large area more than several 10  $\mu\text{m}$ .<sup>6–9</sup> In addition, X-ray scattering are usually applied to analyze the crystallinity and chain axis of crystallites, but amorphous polymers are normally used for optical devices.<sup>10–13</sup> Hence, these techniques are not suitable for the evaluation of the microstructure of amorphous polymers in the localized region of the microscale features such as several 10  $\mu\text{m}$ .

Raman spectroscopy is a useful and simple technique to obtain the information of microstructure in local region, and virtually requires no sample preparation. Because in the measurement of Raman spectroscopy, laser beam of 1–2  $\mu\text{m}$  in diameter is used by adjusting the focus of the microscope lens on the sample stage, this technique can be efficient to characterize microstructure of injection-molded parts with microscale features. Some research groups have investigated the molecular orientation of blow moldings, extruded parts, and injection moldings using polarized Raman spectroscopy.<sup>14–17</sup> However, no

Correspondence to: O. Murakami (kazushi@kit.ac.jp).

study on internal structure of the microscale feature prepared by injection molding using Raman spectroscopy has been found in open literatures.

In this study, polycarbonate (PC) injection-molded parts with v-grooves were molded with different injection molding conditions. Internal structure inside the v-grooves was evaluated by Raman spectroscopy to investigate the relationship between injection molding conditions and the molecular orientation of the injection-molded parts with v-grooves.

## EXPERIMENTAL

### Polymer materials

The polymer materials used in this study were of commercial grade PC, namely Iupilon S2000, supplied by Mitsubishi Engineering-Plastics Corporation (Mie, Japan). This polymer is a standard material for general parts. The weight-average molecular weights were analyzed using a Shimadzu gel permeation chromatography (GPC), model LC-6A (Kyoto, Japan). The values of number-average molecular weight ( $M_n$ ) was 22,800, weight-average molecular weight ( $M_w$ ) was 43,400, and molecular weight distribution ( $M_w/M_n$ ) was 1.90. Glass transition temperatures ( $T_g$ ) of S2000 were analyzed using a Perkin-Elmer differential scanning calorimeter (DSC), model DSC-7 (Osaka, Japan);  $T_g$  was 151°C.

### Mold cavity shape

Figure 1 shows the geometry of the rectangular plate molded parts with single-sided continuous microscale v-groove and located fan-gate at the short side. The dimensions of the molded parts are  $43 \times 35$  mm<sup>2</sup> and the thickness is 1.0 mm. The microscopic v-groove features include 20 μm in depth and 50 μm in width in the molded parts. The direction of v-groove was parallel to the flow direction.

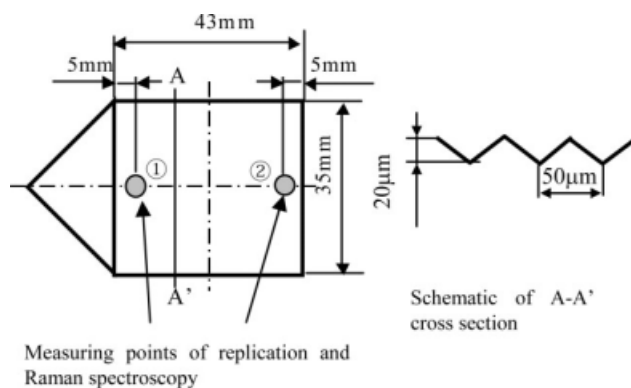


**Figure 1** Cavity shape and measuring points.

**TABLE I**  
Injection Molding Conditions

Condition	Melt temperature (°C)	Mold temperature (°C)	Injection velocity (mm/s)	Holding pressure (MPa)
1	300	120	200	40
2	280	120	200	40
3	320	120	200	40
4	300	100	200	40
5	300	140	200	40
6	300	120	100	40
7	300	120	300	40
8	300	120	200	20
9	300	120	200	80

### Injection molding

Injection-molded parts were produced using a Nissei TH80E injection molding machine (Nagano, Japan). Injection molding conditions are listed in Table I. The melt temperature, mold temperature, injection velocity, and holding pressure were systematically changed in three levels.

### Evaluation of replication

For evaluating replication of the injection molded parts with microscale v-groove, the dimensions were measured using a noncontact 3D laser measuring system, Mitaka Kohki NH-3 (Tokyo, Japan), and compared with dimensions of the mold cavity. The replication was defined as follows;

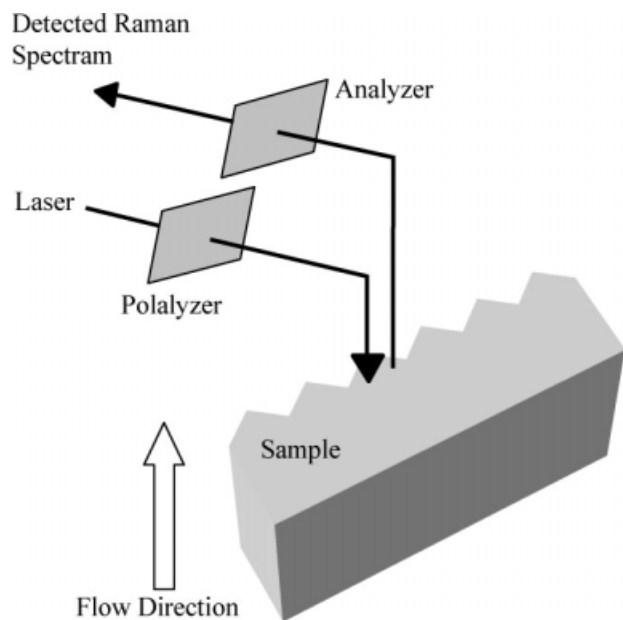
$$\text{Replication}(\%) = \frac{H_m}{H_0} \times 100$$

where  $H_m$  is the height of the injection-molded parts and  $H_0$  is the height of the mold cavity. The replicated features of the v-groove were observed using a JEOL SM-6630F scanning electron microscopy (SEM) (Tokyo, Japan).

### Raman spectroscopy

For Raman spectroscopy investigations, the injection-molded rectangular plates were cut perpendicular to the v-groove direction (flow direction) at the two positions, which is near the gate and far from the gate as shown in Figure 1. To minimize the damage caused by the cutting process, the samples were prepared using a microtome (Rotary Microtome HM355, Carl Zeiss).

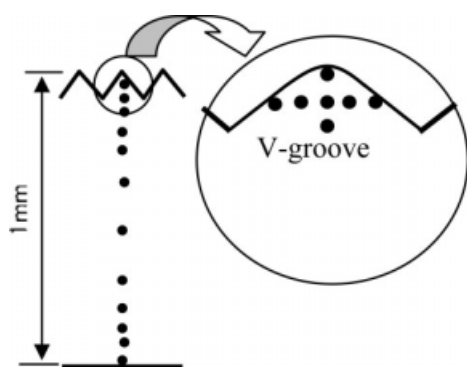
Molecular orientation of injection-molded parts of PC has been analyzed by using Raman spectroscopy, and the equipment scheme is shown in Figure 2. Raman spectra were collected using a RAMASCOPE



**Figure 2** Measuring points along the v-groove cross-section by Raman spectroscopy.

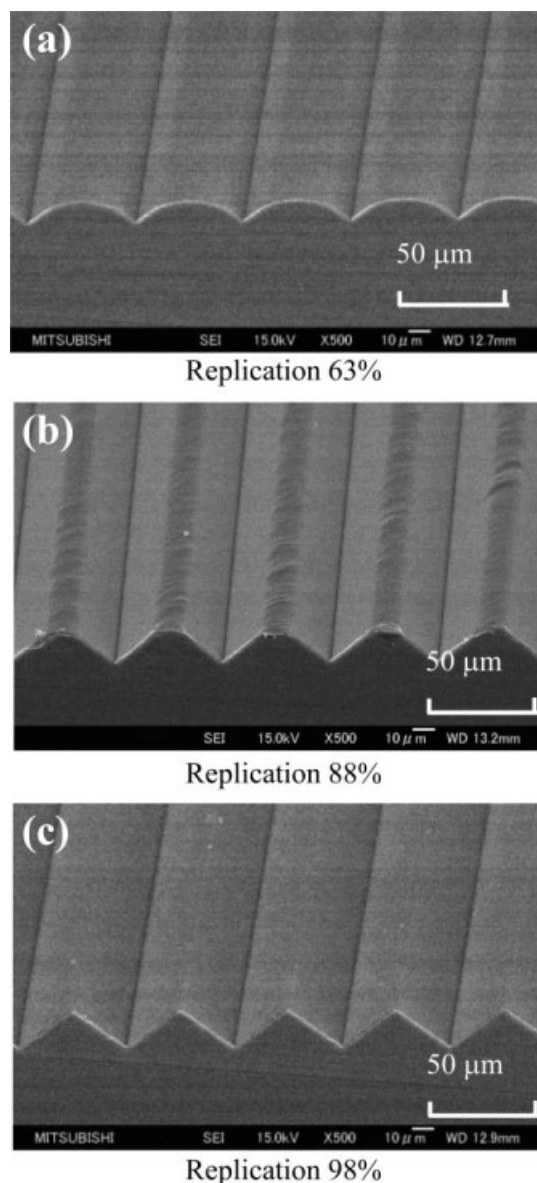
Raman microscope made by Renishaw (Nagoya, Japan). The main components of the system were a 514 nm  $\text{Ar}^+$  laser, a fiber optic probe head, an imaging spectrograph, a CCD camera, and a microscope (Olympus BH2-UMA). The microscope was used to focus the incident laser beam to a 2- $\mu\text{m}$  spot on the sample surface. The incident polarized laser of  $\sim 3$  mW was irradiated.

Figure 3 shows the measuring points of the cross section, which is 11 points along the vertical direction from surface of the v-groove to the opposite surface. To investigate inside the v-groove in detail, the surface of the v-groove cross section were measured at the three points in the vertical direction and five points in the horizontal direction. To analyze the molecular orientation in the specimen, an incident polarized laser beam in conjunction with a



**Figure 3** Arrangement of equipment for Raman spectroscopy.

polarization analyzer for the collected Raman scattering was used. The incident laser beam was polarized parallel to the specimens. The scattered light was collected with a propagation direction, and the analyzer was oriented to transmit only light with a polarization parallel to the incident light. The cross section of the specimen was perpendicular to the flow direction. Hence, the direction of polarization of the incident and scattered light are perpendicular to the flow direction. Each spectrum is collected as an average of 10 scans so that the applied parameters result in an optimum Signal/Noise (S/N) ratio for all spectra. A quantitative interpretation of the spectra in the 200–2000  $\text{cm}^{-1}$  frequency range is



**Figure 4** SEM micrographs of injection-molded parts with different replications of v-groove: (a) low replication 63%, (b) middle replication 88%, and (c) high replication 98%.

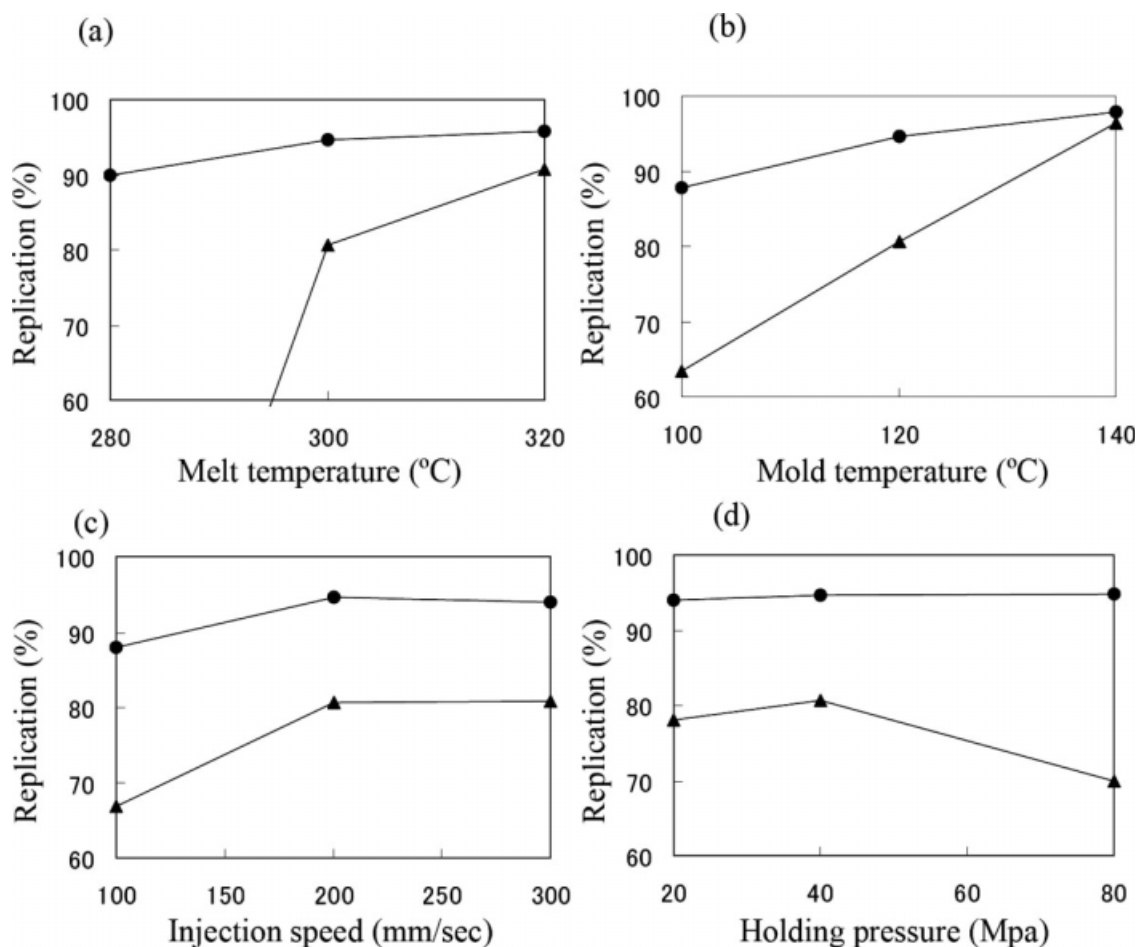


**Figure 5** Relationship between replication and injection molding conditions: (a) melt temperature, (b) mold temperature, (c) injection speed, and (d) holding pressure; ●: Position 1, ▲: Position 2.

made using the baseline theory for correction of the individual spectra.

## RESULTS AND DISCUSSION

### Replication of v-groove

Figure 4 shows typical SEM micrographs of the injection-molded parts with different replications. The shape of v-grooves was not very sharp in the injection-molded parts with replications of 63 and 88%. Figure 5 shows the relationship between replication and injection molding conditions. In Figure 5(a), replication was increased gradually with increasing melt temperature. In the effect of mold temperature on replication [Fig. 5(b)], replication was also gradually increased close to 100% with increasing mold temperature. The replication was achieved at around 98% at both positions near the gate and far from the gate at mold temperature of 140°C, which was around  $T_g$  of PC, i.e., high replication was uniformly obtained in a whole plate with the condition. This might be due to that the filling process of PC resin was completed earlier than the

solidification of PC injected into a mold. Therefore, it is considered that the mold temperature plays an important role to achieve high replication. On the other hand, the relationships between replication and injection speed and holding pressure are shown in Figure 5(c,d). It was found that replication was not significantly affected by injection speed and holding pressure in the tested range.

### Molecular orientation evaluation by Raman spectroscopy

Figure 6 shows typically polarized Raman spectra of PC on the cross-section surface, which is perpendicular to the flow direction of PC injection-molded parts. In the case of PC, main seven characteristic peaks are usually observed in the wide range from 635 to 1600  $\text{cm}^{-1}$  by Raman spectroscopy. Generally, some of the Raman band peaks of PC might be assigned to aromatic rings vibration because the C=C bond has a high symmetry and the vibration mode can be clearly seen in Raman scattering. As reported by Takeshima et al.,<sup>17</sup> Raman band shift of PC is classified into two groups. One is a  $\theta$ -



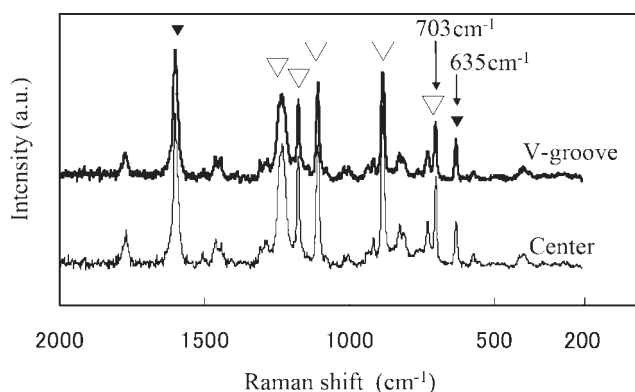


**Figure 6** Raman shift of high replication sample and low replication sample with injection-molded parts using polycarbonate. □: Peak was constant. ▼: Peak was not constant.

dependent group (Raman band peak positions in the range of 703–1235  $\text{cm}^{-1}$ ) and the other is a  $\theta$ -independent group (Raman band peak positions at 635 and 1600  $\text{cm}^{-1}$ ).  $\theta$  is defined as the angle between the polarization direction of the incident laser beam and the axis of molecular orientation. Apparent molecular orientation analysis was performed using the relative intensity ratio of  $\theta$ -dependent group and  $\theta$ -independent group. Therefore, in this study, the adjacent Raman band peaks of 635 and 703  $\text{cm}^{-1}$  were chosen, and then all of Raman spectra were normalized by the intensity at 635  $\text{cm}^{-1}$ . It has been reported that the intensity ratio of the Raman band peaks at 703  $\text{cm}^{-1}$  to that at 635  $\text{cm}^{-1}$  ( $I_{703}/I_{635}$ ) correlates well with the degree of molecular orientation, when the polarized laser is irradiated perpendicular to the flow direction. However, in this study, the polarized laser was irradiated parallel to the flow direction. Thereby, the intensity of Raman scattering bands of 703–1235  $\text{cm}^{-1}$  decreases if polymer main chains are oriented along the flow direction. Indeed, the intensity of the two Raman spectra in Figure 6 was different, and the intensity of spectrum of the oriented (injection moldings) sample was weaker than that of the nonoriented sample at the range of 703–1235  $\text{cm}^{-1}$ . This result well correlates with the general skin-core theory in injection-molded parts; that is, the proportion of molecular orientation in skin layer is higher than that of the core layer in the injection moldings. In this article, we define the reciprocal ratio as the degree of the molecular orientation; namely, the molecular orientation was defined by intensity ratio of the band at 635  $\text{cm}^{-1}$  to that at 703  $\text{cm}^{-1}$  ( $I_{635}/I_{703}$ ).

#### Molecular orientation at the inside of the injection molded parts

The intensity ratios ( $I_{635}/I_{703}$ ) at the different positions in the thickness direction from the v-groove

side to the opposite surface side are plotted in Figure 7. It was clear that the region where intensity ratio ( $I_{635}/I_{703}$ ) was the highest in the injection-molded parts was the inside of v-groove in all the injection molding conditions. This result indicates that the molecular orientation in the v-groove was higher than that in other region such as the core region or the opposite surface region. The intensity ratio ( $I_{635}/I_{703}$ ) near the surface in v-groove was higher than that in the center of the v-groove, and molecular orientation at the tip of the v-groove was the highest in the injection-molded parts. Microstructure of injection-molded parts with microscale features was composed of higher molecular orientation at the skin layer and lower orientation at the core layer. This structure was similar to usual injection-molded parts with multilayered structure.<sup>18</sup> In addition, the intensity ratio ( $I_{635}/I_{703}$ ) decreased from v-groove tip to the center even within v-groove. Generally, in melt state without shear force, a polymer molecule is a random coil entangled with other coiled molecules.

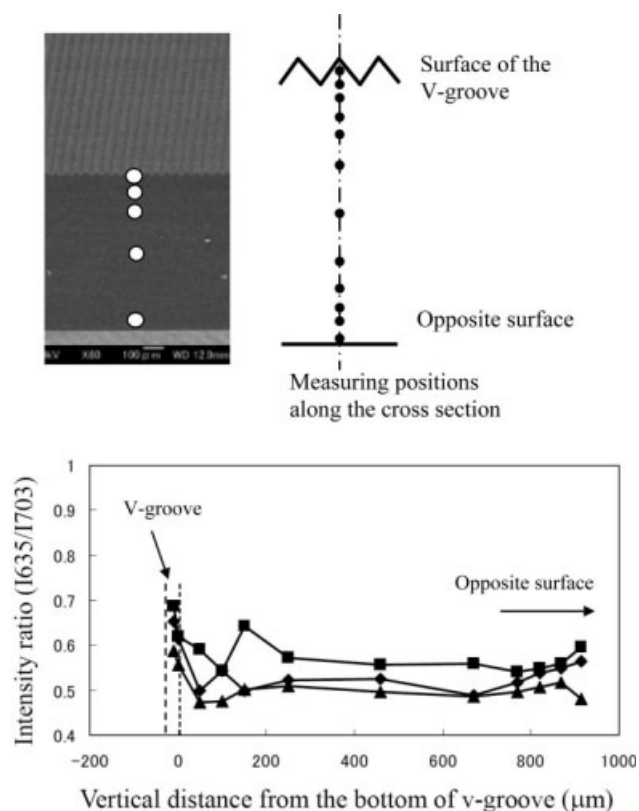


**Figure 7** Intensity ratio of 635 to 703  $\text{cm}^{-1}$  ( $I_{635}/I_{703}$ ) versus difference replication with mold conditions along the cross section from surface of the v-groove to opposite surface. ■: Melt temp: 300°C, Mold temp: 100°C, Injection speed: 200 mm/s, Holding pressure: 40 MP, replication: 88%; ▲: Melt temp: 300°C, Mold temp: 140°C, Injection speed: 200 mm/s, Holding pressure: 40 MP, replication: 98%; ◆: Melt temp: 300°C, Mold temp: 120°C, Injection speed: 300 mm/s, Holding pressure: 40 MP, replication: 99%.

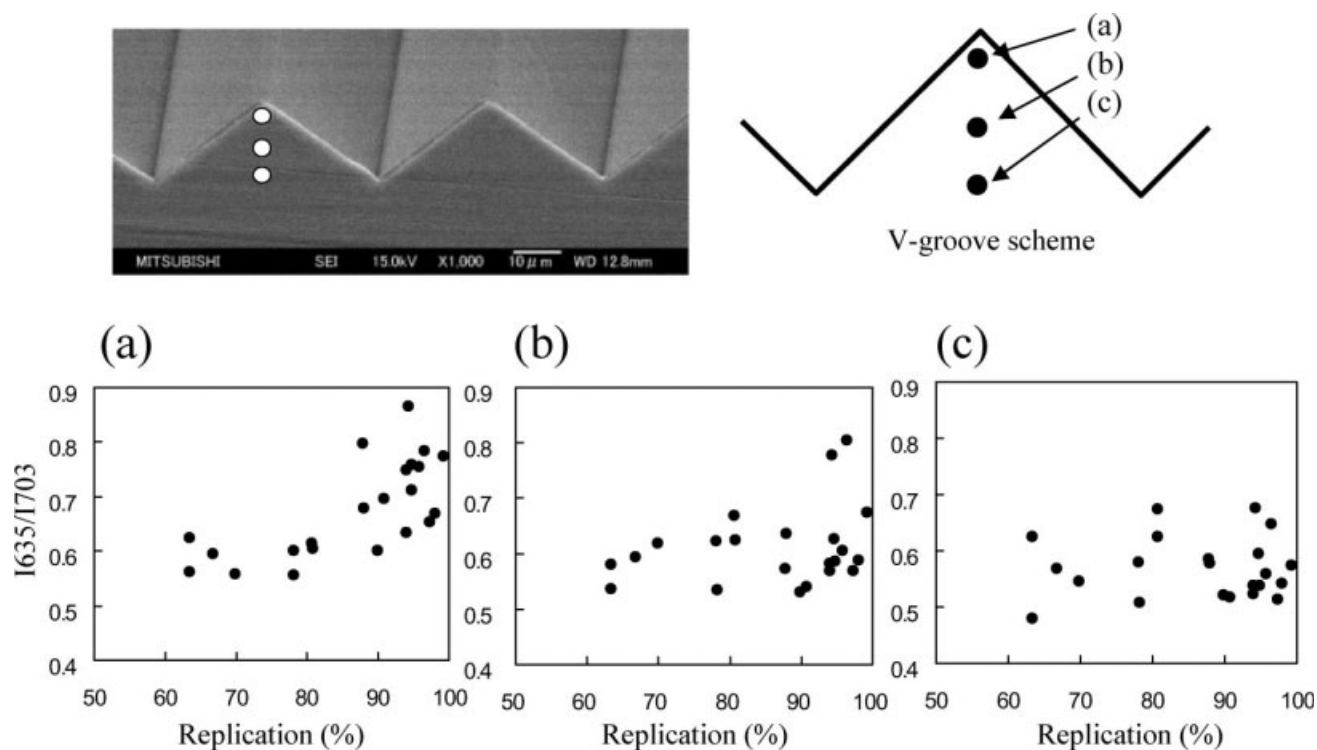


**Figure 8** Relationship between replication and intensity ratio ( $I_{635}/I_{703}$ ) for vertical direction.

High viscosity of polymer melts is due to this entangled structure. In injection molding, shear force pulls molecules from entangled states and aligns them along with neighbors. The shear force generated near mold surface is stronger than that in the core part. This is the reason why the degree of molecular orientation in the skin part is higher than that in the core part. However, in this study, the size of v-grooves was less than  $50\ \mu\text{m}$  and the characterized point size by Raman spectra was approximately a few micrometers. It is noteworthy that the effect of injection molding conditions on molecular orientation was clearly seen in such a small region of v-groove. From Figure 7, in the case of the same high replication 98–99%, the intensity ratio ( $I_{635}/I_{703}$ ) with high injection speed was higher than that with high mold temperature. In addition, the intensity ratio ( $I_{635}/I_{703}$ ) with low mold temperature condition tended to be higher than that with high mold temperature. These results support that the oriented polymer molecules are partially relaxed at higher mold temperature.

#### Molecular orientation at the inside of the v-groove

Figure 8 shows the relationship between intensity ratio ( $I_{635}/I_{703}$ ) and replication at the inside of v-groove in the thickness direction obtained by various molding conditions. Molecular orientation increased

with increasing replication at the tip of the v-groove as shown in Figure 8(a). In Figure 8(b), the tendency of the intensity ratio was almost similar to the case of Figure 8(a), although the intensity ratio of Raman bands was slightly lower at high replication. However, in the case of Figure 8(c), molecular orientation was independent on replication at the deeper position, the intensity ratio of Raman bands was constant within the range of 0.5–0.65.

The relationship between intensity ratio ( $I_{635}/I_{703}$ ) and replication at the inside of the v-groove for horizontal direction at all the molding conditions is shown in Figure 9. Molecular orientation at the hill-side region of the v-groove [Fig. 9(a)] was higher than that of the inside region [Fig. 9(c)]. These results indicate the tendency similar to the results shown in Figure 8. However in this case, higher molecular orientation was obtained even when the replication was lower than 90% as shown in Figure 9(a).

The possible explanation for the difference of the results in Figures 8 and 9 is as follows. When the replication is low (ca. 63%), because polymer is not fully filled into the tip of the v-groove, the shear rate at the tip of the v-groove is not very high and consequently the degree of molecular orientation becomes low. It is considered that the extent of molecular deformation increased at the locations near the mold wall during the filling stage, and then the highly oriented structure developed near the mold wall, but

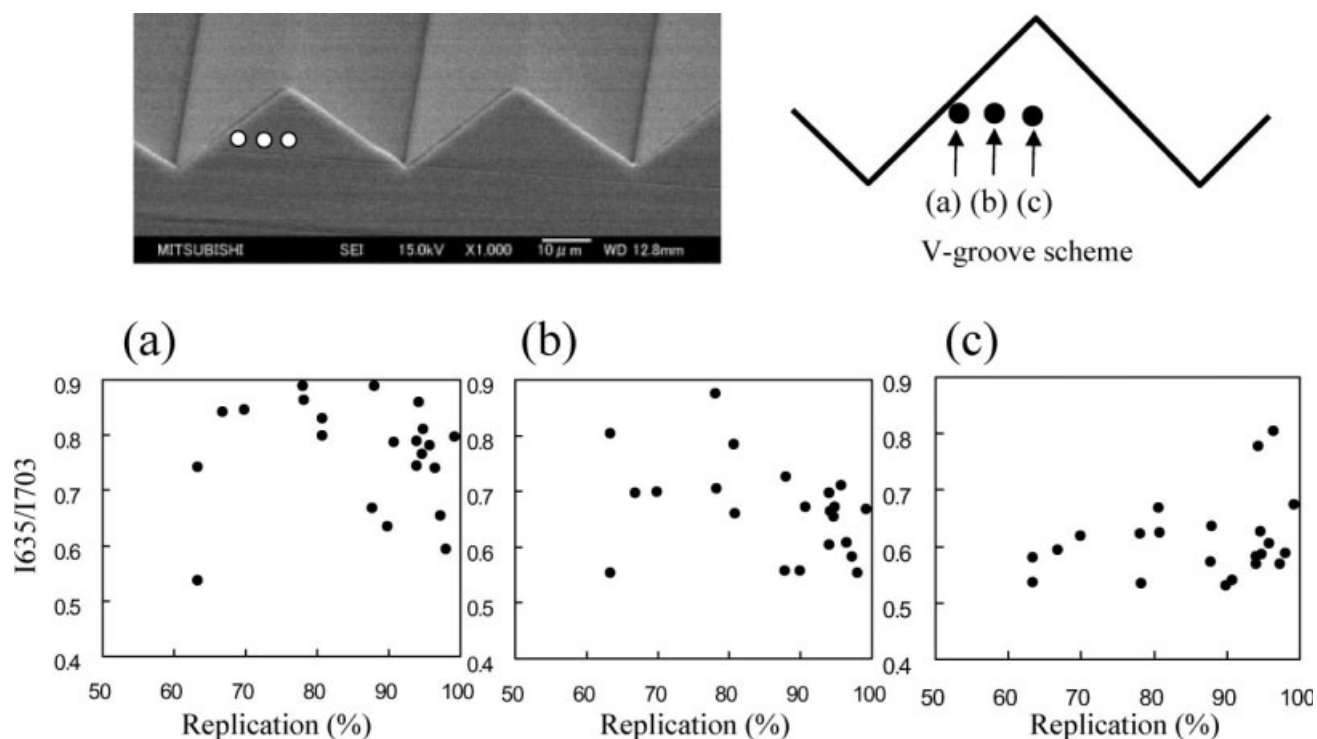


Figure 9 Relationship between replication and intensity ratio ( $I_{635}/I_{703}$ ) for horizontal direction.

the relaxation of molecular chains in the cooling stage might affect the resultant molecular orientation. Hence, it is important to control the process of

the competition between shear deformation and heat relaxation to obtain desired replication and molecular orientation in injection-molded parts.

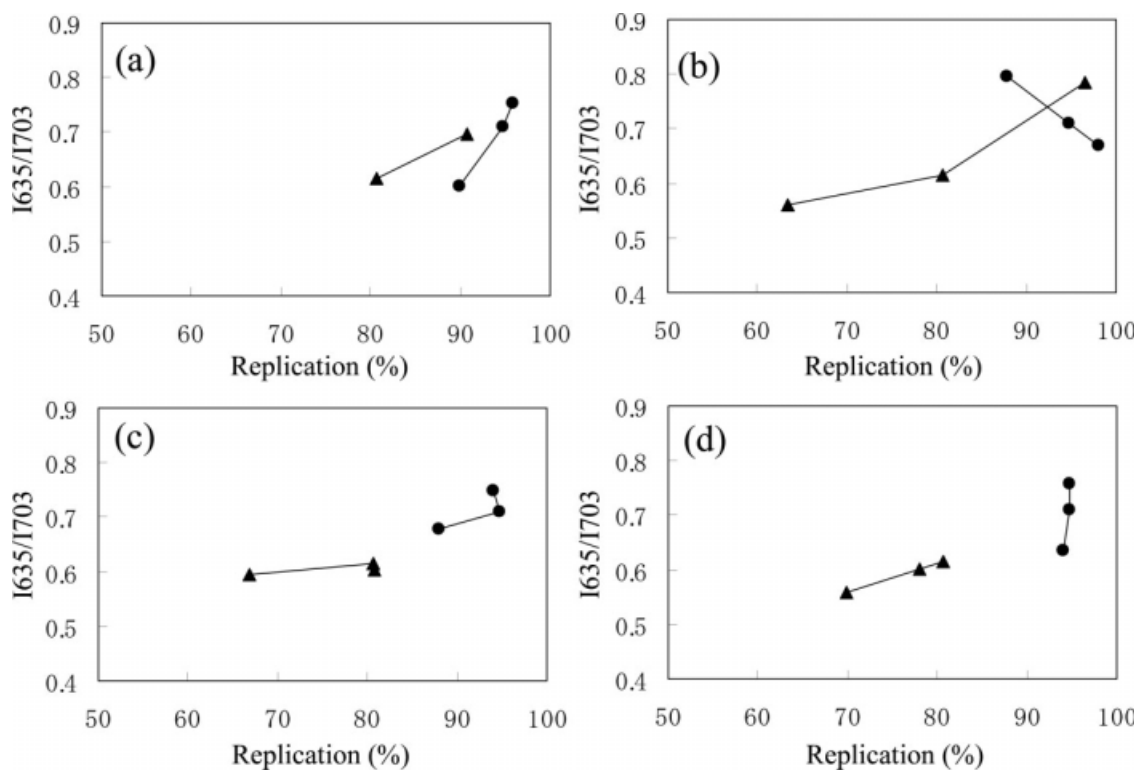


Figure 10 Relationship between replication and intensity ratio ( $I_{635}/I_{703}$ ) at the tip of v-groove with various mold conditions: (a) melt temperature, (b) mold temperature, (c) injection speed, (d) holding pressure; ●: Position 1; ▲: Position 2.

### Relation between injection molding conditions, molecular orientation, and replication

Figure 10 shows the relationship between molecular orientation and replication at the tip of v-groove with various molding conditions. In all the relationships with different molding conditions, molecular orientation tended to increase with increasing replication by changing molding conditions, except mold temperature [Fig. 10(b)]. In addition, the intensity ratio of Raman band peaks and the replication near the gate were higher than those near the flow end. This result means that high shear force was generated to fill polymer into the narrow cavity with microscale features. The effect of mold temperature on the relationship between molecular orientation and replication near the gate [Fig. 10(b)] indicated different trends from the other molding condition effects, i.e., higher mold temperature led to higher replication, but lower molecular orientation. The higher mold temperature caused a longer cooling time during the filling stage, i.e., the extended molecular chains of PC in the injection process were relaxed in the cooling stage. In the case of the lower mold temperature, the polymer contacted with the mold wall surface was solidified faster, and then high molecular orientation near the surface was obtained. It is noteworthy that these phenomena were observed within the v-groove with the size less than 50  $\mu\text{m}$ . We have succeeded in the observation of the phenomenon in the microinjection molded parts at the micron scale by Raman spectroscopy. Further efforts are being made to investigate the molecular orientation–replication relationships in the microinjection-molded parts with different polymers and cavity shapes to understand filling mechanism and achieve superior properties for optical devices.

### CONCLUSION

Molecular orientation of PC along the flow direction of the injection-molded parts with micron scale features characterized by polarized Raman spectroscopy was investigated, and the relationship between molecular orientation and replication was discussed. Molecular orientation was evaluated by the intensity

ratio of the band at 635 to that at 703  $\text{cm}^{-1}$  ( $I_{635}/I_{703}$ ). Molecular orientation was not uniform even in the micron scale v-groove parts, and higher molecular orientation was observed near the surface of the v-groove.

For the relationship between molecular orientation and replication of the v-grooves molded by different injection molding conditions, the injection-molded parts with higher replication tended to have higher molecular orientation. However, higher mold temperature led to higher replication, but lower molecular orientation. The results obtained in this study can be used to understand the filling mechanism in the microinjection-molded parts and optimize injection molding conditions for optical device fabrication where high replication and low molecular orientation are required.

### References

- Gale, M. T.; Gimkiewicz, C.; Obi, S.; Schnieper, M.; Sochtig, J.; Thiele, H.; Westenhofer, S. *Opt Lasers Eng* 2005, 43, 373.
- Su, Y.; Shah, J.; Lin, L. *J Micromech Microeng* 2004, 14, 415.
- Theilade, U. A.; Hansen, H. N. *Int Adv Manuf Technol* 2007, 33, 157.
- Mönkkönen, K.; Hietalala, J.; Pääkkönen, P.; Pääkkönen, E. J.; Kaikuranta, T.; Pakkanen, T. T.; Jääskeläinen, T. *Polym Eng Sci* 2002, 42, 1600.
- Lee, B. K.; Kim, D. S.; Kwon, T. H. *Microsyst Technol* 2004, 10, 531.
- Pirnia, A.; Sung, C. S. P. *Macromolecules* 1988, 21, 2699.
- Kaito, A.; Kyotani, M.; Nakayama, K. *Macromolecules* 1988, 24, 3244.
- Uchiyama, A.; Yatabe, T. *J Polym Sci Part B: Polym Phys* 2003, 41, 1554.
- Pontani, R.; Sorrentino, A.; Speranza, V.; Titomanlio, G. *Rheol Acta* 2004, 43, 109.
- Zipper, P.; Janosi, A.; Geymayer, W.; Ingolic, E.; Fleischmann, E. *Polym Eng Sci* 1996, 36, 467.
- Riekkel, C.; Dieing, T.; Engsröm, P.; Vincze, L.; Martin, C.; Mahendrasingam, A. *Macromolecules* 1999, 32, 7859.
- Kumaraswamy, G.; Issaian, A. M.; Kornfield, J. A. *Macromolecules* 1999, 32, 7537.
- Davis, R. J.; Burghammer, M.; Riekkel, C. *Macromolecules* 2005, 38, 3364.
- Hendra, P. J.; Morris, D. B.; Sang, R. D.; Willis, H. A. *Polymer* 1982, 23, 9.
- Yang, S.; Michielsen, S. *Macromolecules* 2003, 36, 6484.
- Natarajan, S.; Michielsen, S. *J Appl Polym Sci* 1999, 73, 943.
- Takeshima, M.; Funakoshi, N. *J Appl Polym Sci* 1986, 32, 3457.
- Guo, X.; Isayev, A.; Guo, L. *Polym Eng Sci* 1999, 39, 2096.